Published in final edited form as:
Alzheimers Dement. 2012 January ; 8(1): 51–59. doi:10.1016/j.jalz.2011.06.003.

Direct Comparison of FDG-PET and ASL-MRI in Alzheimer's Disease

Erik S. Musiek[1], **Yufen Chen**[2], **Marc Korczykowski**[2], **Babak Saboury**[3], **Patricia M. Martinez**[4], **Janet S. Reddin**[3], **Abass Alavi**[3], **Daniel Y. Kimberg**[2], **David A. Wolk**[1], **Per Julin**[5], **Andrew B. Newberg**[3], **Steven E. Arnold**[4], and **John A. Detre**[1,2,3]

[1]Department of Neurology, University of Pennsylvania, 3400 Spruce St., Philadelphia, PA 19104

[2]Center for Functional Neuroimaging, University of Pennsylvania, 3400 Spruce St., Philadelphia, PA 19104

[3]Department of Radiology, University of Pennsylvania, 3400 Spruce St., Philadelphia, PA 19104

[4]Department of Psychiatry, University of Pennsylvania, 3400 Spruce St., Philadelphia, PA 19104

[5]AstraZeneca R&D, Västra Mälarehamnen 9, Södertälje, Sweden, SE-151 85

Abstract

BACKGROUND—The utility flourodeoxyglucose PET (FDG-PET) imaging in Alzheimer's Disease (AD) diagnosis is well established. Recently, measurement of cerebral blood flow using arterial spin labeling MRI (ASL-MRI) has shown diagnostic potential in AD, though it has never been directly compared to FDG-PET.

METHODS—We employed a novel imaging protocol to obtain FDG-PET and ASL-MRI images concurrently in 17 AD patients and 19 age-matched controls. Paired FDG-PET and ASL-MRI images from 19 controls and 15 AD patients were included for qualitative analysis, while paired images 18 controls and 13 AD patients were suitable for quantitative analyses.

RESULTS—The combined imaging protocol was well tolerated. Both modalities revealed very similar regional abnormalities in AD, as well as comparable sensitivity and specificity for the detection of AD following visual review by two expert readers. Interobserver agreement was better for FDG-PET (kappa 0.75, SE 0.12) than ASL-MRI (kappa 0.51, SE 0.15), intermodality agreement was moderate to strong (kappa 0.45-0.61), and readers were more confident of FDG-PET reads. Simple quantitative analysis of global cerebral FDG uptake (FDG-PET) or whole brain cerebral blood flow (ASL-MRI) showed excellent diagnostic accuracy for both modalities, with area under ROC curves of 0.90 for FDG-PET (95% CI 0.79-0.99) and 0.91 for ASL-MRI (95% CI 0.80-1.00).

CONCLUSIONS—Our results demonstrate that FDG-PET and ASL-MRI identify similar regional abnormalities and have comparable diagnostic accuracy in a small population of AD patients, and support the further study of ASL-MRI in dementia diagnosis.

Corresponding Author: Dr. John Detre, Center for Functional Neuroimaging, Univ. of Pennsylvania, 3 Gates, 3400 Spruce St., Philadelphia, PA, 19104. detre@mail.med.upenn.edu.

The other authors report no conflicts of interest and have nothing to disclose.

Keywords

ASL; FDG; PET; MRI; Alzheimer's disease; spin label; fluorodeoxyglucose; dementia

1. INTRODUCTION

Considerable effort over the past 20 years has been targeted at the improved diagnosis of Alzheimer Disease (AD). Regional hypometabolism on positron emission tomographic imaging with [^{18}F]-fluorodeoxyglucose (FDG-PET) has been well established as a marker of AD (1-4). However, enthusiasm for FDG-PET in AD diagnosis and monitoring has been mitigated by limited availability, radiation exposure, and expense.

Arterial spin labeling perfusion MRI (ASL-MRI) uses magnetically labeled arterial blood water as a tracer (5), and has emerged as a noninvasive and reliable modality for quantitative measurement of regional cerebral blood flow (CBF) (6). Since regional CBF and glucose metabolism are generally tightly coupled (7), regional ASL-MRI measures of CBF are expected to closely parallel metabolic changes seen with FDG-PET. Indeed, several groups have demonstrated that ASL-MRI can differentiate AD or mild cognitive impairment patients from controls (8-14). ASL-MRI can be performed alongside structural MRI sequences during the routine dementia workup and requires no exogenous contrast or radiation exposure. Thus, ASL represents a potentially appealing functional imaging modality for AD diagnosis and monitoring. To date, however, no studies have directly compared ASL-MRI to FDG-PET in AD patients. Herein, we compare FDG-PET and ASL-MRI imaging in a cohort of AD patients and controls. To eliminate physiological variability between FDG-PET and ASL-MRI scans, we employed a novel methodological approach in which FDG is administered during the acquisition of ASL-MRI (15), providing concurrent measurements of regional CBF and metabolism.

2. METHODS

2.1. Subjects

17 subjects with clinically-diagnosed AD and 19 cognitively normal controls were recruited from the cohort of the Penn Memory Center/ Alzheimer's Disease Center. Ultimately, paired ASL-MRI and FDG-PET images from all 19 controls and 15 AD patients were included for qualitative analysis (expert reader diagnosis, sensitivity, specificity, kappa, and ischemic burden analyses), and paired images from 18 controls and 13 AD patients were included for quantitative analyses (FDG SUV ratio, ASL CBF, ROC curve analysis). Control and AD patients were matched for age and years of education (Table 1). All patients underwent full neurocognitive assessment, including all elements of the National Alzheimer's Coordinating Center's Uniform Data Set that is conducted by all National Institute of Aging-sponsored Alzheimer Disease Centers (16). All controls had a Clinical Dementia Rating (CDR) of 0 and a mini mental status score (MMSE) > 27, and all clinically diagnosed AD patients included in the study had a CDR of 0.5 or more, and an MMSE less than 25 (Table 1). The mean CDR for AD patients was 1.04±0.72. Exclusion criteria included age <50 or >80, history of stroke or other known intracranial abnormality, clinically relevant abnormalities on routine bloodwork including glucose > 200, contraindication to MRI or PET, and history of Axis I psychiatric disease or substance abuse. All scans were performed between December 2008 and November 2009, and current MMSE testing was performed on all patients during that interval.

2.2. Imaging Protocol

In order to most closely correlate ASL-MRI findings with FDG-PET, a unique imaging protocol was employed. At the initiation on the ASL-MRI scan, while in the scanner, 5mCi of FDG was injected via intravenous catheter, such that FDG uptake and ASL imaging occurred simultaneously. PET imaging was then performed 40 minutes later.

2.3. MRI Imaging

3T high resolution T1-weighted images were acquired using MPRAGE (17). ASL images were acquired with pseudo-continuous labeling (mean Gz=0.6mT/m, 1640 Hanning window-shaped radiofrequency (RF) pulses for a total labeling duration =1.8s, RF duration=500μs, RF gap=360μs, postlabeling delay=1.5s) and gradient-echo echo-planar imaging . Imaging parameters for ASL include TE/TR=17ms/4s, image resolution=3.4×3.4×6mm^3, 18 axial slices with 1mm gap prescribed to cover the entire brain. An ascending acquisition order was used, and ramp sampling was used employed with a readout bandwidth was 3004Hz/voxel. All 18 slices were acquired during the same acquisition sesion. Each ASL scan consisted of 59 pairs of interleaved control and tag images, and three ASL scans were concatenated to improve signal-to-noise ratio.

ASL and structural images were coregistered using SPM5 (The Wellcome Department of Imaging Neuroscience, London, UK). Pairwise subtraction images were generated and averaged using in-house developed Matlab (The Mathworks Inc., Natick, MA, USA) script. These were converted to quantitative CBF maps in units of ml/100g/min based on a single compartment ASL model (18), then spatially normalized to Montreal Neurological Institute (MNI) space with 2mm isotropic resolution and smoothed with an isotropic kernel of 8mm to facilitate comparison with the similarly normalized PET images. CBF measurements represent whole-brain CBF values with no partial volume correction or grey matter coregistration.

2.4. FDG-PET Imaging

PET imaging was carried out based on the ADNI PET imaging protocol (19). At the initiation of the ASL scan, patients were injected with FDG. PET imaging was initiated 40 minutes after the administration of FDG, and was conducted in a darkened, quiet room. Images were obtained on an Allegro scanner (Philips). Images were reconstructed in the transaxial plane using iterative reconstruction and ^{137}Cesium transmission scan for attenuation correction.

The whole brain standardized uptake value ratio was determined by defining an automated volume of interest encompassing the entire brain parenchyma with an intensity >25% of the maximal voxel intensity. The mean SUV for the whole brain was determined automatically, and divided by the mean SUV of a volume of interest encompassing one cerebellar hemisphere.

2.5. Qualitative Analysis

Each ASL-MRI and FDG-PET image was independently reviewed in a blinded manner by two expert nuclear medicine physicians with >10 years experience reading functional brain images. The readers did not see the structural MRI images. The readers then reread the image set several months later, again in a blinded fashion. The readers made a forced-decision diagnosis (AD or control) for each patient with each modality, and also evaluated 14 regions (frontal, temporal, parietal, occipital lobes, basal ganglia, thalamus, and cerebellum; right and left) and scored them from 1-4, with the following scoring criteria: 4-normal, 3 -mildly decreased, 2-moderately decreased, 1-severely decreased. These criteria

and the regions of interest were defined during a short instructional session with the readers, after which several trial images were evaluated using the criteria.

2.6. Quantification of White Matter Ischemic Burden

Axial FLAIR MRI images, obtained during the ASL imaging session, were visually assessed and scored for white matter ischemic burden by a separate blinded reader based on the criteria of Erkinjuntti et al. (20). The scorer was a physician with experience in MRI interpretation and was blinded to diagnosis. Scoring was based on the appearance of the subcortical and deep white matter, and images were scored on a 0-4 scale, with 0=no ischemic changes, 1= < 5 small (<5mm diameter in largest dimension) and < 2 large (>2cm in diameter in largest dimension) FLAIR-positive lesions, 2= 5-12 small lesion or 2-4 large, 3= >12 small or >4 large or focal areas of confluent white matter injury, and 4=predominantly confluent white matter injury.

2.7. Statistical Analysis

Receiver-Operator curve (ROC) analysis, t-tests, and sensitivity/specificity analysis were performed using GraphPad Prizm version 4.00 for Windows (GraphPad Software, San Diego California). Mean values of FDG SUV ratio and ASL CBF were compared between controls and AD patients by unpaired two-tailed T-test. Variances were not significantly different between controls and AD patients ($F(17,12)=1.289$, $p=0.33$). Area under the curve (AUC) and the standard error and statistical significance of each ROC curve was determined automatically by the software using a method based on the non-parametric Mann-Whitney U statistic as described previously (21). The AUCs of FDG-PET ratio and ASL-MRI were compared statistically using MedCalc version 11.3.6 (MedCalc software, Mariakerke, Belgium), which employs the method described by Hanley and McNeil (22). Cohen's kappa statistics were also calculated using MedCalc. An additional analysis to calculate the confidence interval surrounding the difference between AUC measures was performed using the method described by DeLong et al. (23).

3. RESULTS

3.1. Tolerability of Concurrent ASL-MRI/FDG-PET Imaging Protocol

The concurrent FDG-PET and ASL-MRI protocol was well tolerated, and produced interpretable images for both modalities. There were 36 patients who were enrolled in the study and underwent imaging (19 control, 17 AD). There were 2 subjects (both AD patients) that had to be excluded from both qualitative analyses (calculation of sensitivity, specificity, kappa, ischemic burden), subject #11 (FDG PET not usable due to movement artifact) and #16 (patient could not tolerate ASL MRI image acquisition). Thus, qualitative reads were performed on all controls (19), and all but 2 AD patients (15), and each patient had both ASL and FDG data. For quantitative analysis (calculation of FDG SUV ratio, ASL CBF, ROC curves) subjects #11 and 16 were again excluded (for lack of paired FDG and ASL data), as were 3 more patients with incomplete FDG data (#1,2, and 33) who had FDG PET images which could not be used to calculate SUVs. Thus, 18 control and 13 AD patients, all with paired FDG and ASL data, were included in these analyses.

3.2. Qualitative Comparison of ASL-MRI and FDG-PET images

As demonstrated in Fig. 1, images obtained from AD patients using ASL-MRI very closely approximated those obtained with FDG-PET. On visual inspection, the pattern of hypoperfusion on ASL-MRI was generally similar to that of hypometabolism on FDG-PET, with classically affected regions such as the temporal and parietal lobes showing deficits with both modalities. These abnormalities did not appear to be related to structural

abnormalities on T1 MRI or to FLAIR hyperintensities. Regional image intensity was quantified by two expert readers, and was significantly decreased for both modalities in the temporal and parietal lobes in AD patients (Fig. 2). On average, significant frontal lobe hypometabolism was seen using FDG-PET, but this did not reach statistical significance on ASL-MRI. This is in contrast to recent work by Raji et al., which showed prominent frontal hypoperfusion on ASL-MRI in AD (14). However, by visual inspection, there was striking similarity between concurrent FDG-PET and ASL-MRI images in both AD patients and controls.

In our small sample, qualitative expert scoring demonstrated quite similar sensitivity and specificity between the two modalities. According to reader 1, ASL-MRI was slightly more sensitive than FDG-PET (73.3% for FDG (95% CI 44.9-92.2) vs. 80.0% for ASL (95% CI 51.9-95.7)), while FDG was slightly more specific (94.7% for FDG (95% CI 74.0-99.9) vs. 89.4% (95% CI 66.9-98.7) for ASL). Reader 2 had a lower sensitivity (60.0% for FDG (95% CI 32.3-83.7) vs. 46.7% for ASL (95% CI 21.3-73.4), but had very high specificities for both modalities (100% for FDG (95% CI 66.4-100) vs. 94.7% for ASL (95% CI 73.9-99.9), with a modest advantage of FDG in both cases. While the readers varied in their personal thresholds for detection, the performance of FDG-PET and ASL-MRI was quite similar, with substantial overlap of all confidence intervals. When comparing between ASL and PET, Reader 1 demonstrated 73.5% agreement, while Reader 2 had 85.3% agreement. When comparing between readers for a given modality, there was 86.7% agreement for FDG-PET, and 76.5% agreement for ASL-MRI. Cohen's Kappa statistics were calculated to determine interobserver reliability and agreement between modalities for a given observer. The interobserver kappa for FDG-PET was 0.74 (SE 0.12, 95% CI 0.501 to 0.970, moderate-strong agreement), while the interobserver kappa for ASL-MRI was 0.48 (SE 0.15, 95% CI 0.194 to 0.768, moderate agreement). The intermodality kappa for reader 1 was 0.45 (SE 0.16, 95% CI 0.141 to 0.754, moderate agreement) and 0.61 for reader 2 (SE 0.16, 95% CI 0.299 to 0.917, moderate-strong agreement). These statistics suggest that the agreement between observers was slightly better for FDG-PET than ASL-MRI, and the agreement between modalities is only moderate. The readers then examined the images in a consensus fashion, and were asked to denote uncertainty about each diagnosis. The readers marked 4/35 (11.4%) reads as uncertain for FDG-PET, and 11/35 (31.4%) for ASL-MRI. Thus, reads of ASL-MRI images were slightly less consistent over time, and the readers were less confident in the reads of ASL-MRI images. Finally, the same readers examined each study again in a blinded fashion several months later. The intraobserver reliability between sessions was 91.4% for FDG-PET and 82.9% for ASL-MRI.

3.3. Quantitative Comparison

Previous work has shown that global decreases in cerebral FDG uptake can distinguish between AD and normal controls (24). We thus examined the potential clinical value of whole-brain ASL CBF measurement, and compared this to FDG whole brain SUV ratio, which provides a rough estimate of whole brain metabolism. As shown in Fig. 3a, mean ASL-MRI whole brain CBF values were 30.1% lower in AD than control (35.9 vs. 24.5, $t(29)=4.95$, $p<0.001$ by unpaired two-tailed t-test). FDG-SUV ratio was also significantly lower in AD than controls (Fig. 3b), though the magnitude of difference was smaller (16% difference, 0.912 control vs. 0.785 AD, $t(29)=4.40$, $p<0.001$ by unpaired two tailed t-test). As shown in Fig. 3c and d, the areas under the ROC curves for the two modalities were 0.91 (standard error 0.050, $p<0.001$, 95% confidence interval 0.80-1.00) for ASL-MRI CBF, and 0.90 (standard error 0.055, $p<0.001$, 95% confidence interval 0.79-0.99) for FDG-PET SUV ratio. The two AUCs were not significantly different ($z=0.141$, $p=0.89$). The lower bound on the 2 standard deviation confidence interval surrounding the difference between AUC measures from ASL and FDG is −0.104 (a small advantage for FDG), the upper bound was

0.138 (a small advantage for ASL). These results suggest that a given AD patient will have a 91% (for ASL) or a 90% (for FDG) chance of having a lower test value than a given control patient. We selected optimal ASL-MRI CBF cutoff point for AD discrimination by examining a table of potential cutoff points and selected that with the highest calculated likelihood ratio. For ASL-MRI, a cutoff of <31.9 yielded a sensitivity of 77.8% and a specificity of 92.3% with a likelihood ratio of 10.1. For the FDG-PET SUV ratio analysis we chose an optimal cutoff value of <0.86, with a likelihood ratio of 9.1. Using this criterion, FDG-PET SUV ratio had a sensitivity of 72.2% and a specificity of 92.3%. Thus, both quantitative measures performed well in distinguishing AD from control, with neither ASL-MRI nor FDG-PET demonstrating a clear advantage.

3.4. Quantification of Ischemic Burden

In order to evaluate whether differences in white matter ischemic burden differed between groups and might act as a confound, we scored the FLAIR MRI images from each patient for white matter (WM) ischemic injury based on the criteria of Erkinjuntti et al. 20). There was no significant difference between groups in the WM ischemic burden score (1.17±1.20 for controls, 1.36±1.28 for AD patients, $t(29)=0.45$, $p=0.66$ by two-tailed unpaired t-test). Furthermore, visual comparison of the FLAIR, FDG, and ASL images demonstrated that areas of hypoperfusion and hypometabolism did not overlap consistently with FLAIR-positive lesions (see Fig. 1). We concluded that chronic ischemic disease did not likely represent a substantial confound in this cohort.

4. DISCUSSION

Herein we describe an exploratory study aimed at obtaining concurrent ASL-MRI and FDG-PET images using a novel protocol in a small group of patients with AD and age- matched controls, as these modalities have never been directly compared. The concurrent imaging protocol was well tolerated. The most striking finding was the similarity upon visual inspection of the patterns of CBF on ASL-MRI and metabolism on FDG-PET, as depicted in Figure 1. The finding that perfusion and metabolism images resemble one another so closely suggests that these processes remain at least grossly coupled in the brain of Alzheimer's patients. We have characterized this similarity further through qualitative expert analysis and simple whole-brain quantification. Qualitative analysis yielded similar sensitivity and specificity for AD detection for both ASL-MRI and FDG-PET in this small sample, though there was only moderate to good interobserver and intermodality agreement. Quantitative measurement of CBF and FDG SUVs generated ROC curves with AUCs of approximately 90% for both modalities. The 2 standard deviation confidence interval surrounding the difference between the two methods (calculated using the method of (23)) included only small advantages in either direction -- at most a 10.4% accuracy advantage for FDG or a 13.8% advantage for ASL. Thus, this pilot study provides initial data suggesting considerable qualitative and quantitative similarity between ASL-MRI and FDG-PET in AD.

The qualitative similarity of the regional distribution of decreased CBF and diminished FDG uptake in images obtained concurrently in our study suggests that CBF closely parallels glucose metabolism in AD brain. However, the intermodality agreement (kappa statistic) was in the moderate range for both readers, suggesting that while there is considerable similarity between the two modalities, they can produce some diagnostic disparities. This is emphasized by the fact that significant frontal lobe hypoperfusion was noted on FDG-PET, but not on ASL-MRI, a finding which conflicts with a previous report (14). The fact that both readers had extensive experience with FDG-PET but not with ASL-MRI images may explain why the intraobserver reliability and diagnostic confidence was lower for ASL-MRI, but the quantitative analysis was nearly identical. Readers may apply pattern recognition

derived from years of FDG-PET analysis to ASL-MRI images, which are not identical. Further research and clinical experience will be needed to more formally define the patterns of change on ASL-MRI that associate with AD, and to determine the etiology of the heterogeneity that exists between ASL-MRI and FDG-PET.

Discrepancies between ASL-MRI and FDG-PET images could have two potential sources: image artifact, or true perfusion-metabolism mismatch. Perfusion imaging modalities such as ASL-MRI are susceptible to artifact in the setting of vascular compromise, such as arterial stenosis. We found no difference between groups in white matter ischemic changes and focal infarcts on the FLAIR MRI images, but this method is not perfect, and fixed perfusional deficits which did not lead to FLAIR-positive lesions might explain some of these discrepant diagnoses. The readers reported difficulty interpreting several ASL-MRI images due to small areas of hypoperfusion in the parieto-occipital junction, which could be confused with biparietal hypometabolism (Fig. 4). This may be due to decreased perfusion in the watershed zone between anterior and posterior arterial circulations. They also felt that it was more difficult to thoroughly examine the inferior temporal lobes, possibly due to diminished image quality from temporal bone artifact. Despite these issues, regional scoring of temporal lobe image intensity was similar between ASL and FDG, suggesting that these artifacts had minimal impact on diagnosis. It appears likely that these and perhaps other limitations of ASL-MRI images will need to be considered by expert readers, and that accurate diagnosis of AD in larger populations will require diagnostic criteria that are specific to ASL-MRI, and not simply adopted from FDG-PET. The qualitative similarity between ASL-MRI and FDG-PET images suggest that perfusion and metabolism are matched to some degree in AD, but no quantitative measures of regional perfusion or metabolism were made in this study to examine this definitively. Such efforts are in progress. A mismatch between oxygen uptake and glucose metabolism has been recently described in AD-susceptible brain regions in both normal controls and AD patients, and has been attributed to increased aerobic glycolysis in these vulnerable areas (25, 26). It remains to be seen if regional discrepancies between ASL-MRI and FDG-PET are due to this phenomenon.

For the purposes of this report, we chose to focus on image analysis methods that might be accessible to the real-world radiologist, such as visual interpretations and basic whole-brain CBF quantification, as the primary advantages of ASL-MRI over FDG-PET center around convenience, cost, and clinical accessibility. Only a few groups have examined global CBG as a predictor of AD. Asllani et al. showed a 40% decrease in global grey matter-corrected CBF in AD patients (10), while Yoshiura et al showed a 24% decrease without segmentation (13). Our study showed a 31.8% decrease in whole brain CBF (without grey matter correction) in AD, suggesting that our simple, clinically-applicable method is sufficiently sensitive to capture global hypoperfusion in AD. Future work should also compare regional CBF and FDG uptake at the voxel level.

This study has several limitations. It was an exploratory study intended to evaluate a novel imaging method for the concurrent acquisition of FDG-PET and ASL-MRI data, and to determine if FDG-PET and ASL-MRI produce comparable images when performed concurrently in AD patients. The study was not prospectively powered to provide definitive sensitivity and specificity data for these modalities in AD, nor to determine statistical superiority of one modality (or equivalence, although we note that the confidence interval surrounding the AUC difference is fairly narrow). Extrapolating from our sample, if we wanted to narrow this confidence interval down to a worst case of a 5% advantage for FDG, a future study would need to increase our sample size by a factor of 3.11 (40 controls and 56 AD patients). ASL-MRI imaging of approximately 250 patients including patients with AD, MCI, and controls will occur as part of the second phase of the Alzheimer's Disease

Neuroimaging Initiative (ADNI). These data will allow more rigorous statistical appraisal of the diagnostic efficacy of this modality (27). The current work provides further motivation for such rigorous comparison of FDG PET with ASL MRI.

The diagnosis of AD, used as the gold standard in this study, was made on clinical grounds, and can thus not be definitively confirmed without autopsy data, though ASL-MRI data in autopsy confirmed AD has recently been reported (28). Conversely, some recent studies suggest that changes in cerebral metabolism in cognitively normal patients may precede the clinical appearance of cognitive deficits (29, 30), therefore some control subjects could also have had presymptomatic AD. Finally, the sample contained only AD patients and controls, and the results thus cannot be directly applied to the clinical setting, in which a mix of neurodegenerative and dementing illnesses are present.

In summary, we have compared FDG-PET and ASL-MRI images in a population of AD patients and cognitively normal controls using a concurrent protocol to ensure optimal head to head comparison. Our findings suggest that in this small but well-defined population, ASL-MRI yields very similar image patterns and comparable diagnostic accuracy as FDG-PET. While analysis of ASL-MRI images was slightly less consistent than that of FDG-PET, quantitative analysis for both modalities was nearly identical. Considering the many potential advantages of ASL-MRI, our results further bolster the potential utility of this image modality for the diagnosis of AD, and reinforce the need for further efforts to standardize and validate ASL-MRI methods in larger populations of mixed neurodegenerative conditions.

Acknowledgments

This work was support by a grant from the Penn-AstraZeneca Alliance and by NIH grants NS058386, RR002305, and MH080729. Dr. Detre is an inventor on the University of Pennsylvania's patent for ASL-MRI and is entitled to institutional royalty-sharing for its licensure. Dr. Julin is a full-time employee of AstraZeneca, but has no financial disclosures associated with this project.

Abbreviations

AD	Alzheimer's disease
ADNI	Alzheimer's Disease Neuroimaging Initiative
ASL	arterial spin labeling
CDR	clinical dementia rating
CBF	cerebral blood flow
FDG	^{18}F-deoxyglucose
MMSE	mini-mental status evaluation
MRI	magnetic resonance imaging
PET	positron emission tomography
ROC	receiver-operator characteristic
SUV	standardized uptake value

REFERENCES

1. Fazekas F, Alavi A, Chawluk JB, Zimmerman RA, Hackney D, Bilaniuk L, et al. Comparison of CT, MR, and PET in Alzheimer's dementia and normal aging. J Nucl Med. 1989; 30:1607–1615. [PubMed: 2795200]

2. Kumar A, Newberg A, Alavi A, Berlin J, Smith R, Reivich M. Regional cerebral glucose metabolism in late-life depression and Alzheimer disease: a preliminary positron emission tomography study. Proc Natl Acad Sci USA. 1993; 90:7019–7023. [PubMed: 8346211]
3. Silverman DH, Small GW, Chang CY, Lu CS, Kung De, Aburto MA, Chen W, et al. Positron emission tomography in evaluation of dementia: Regional brain metabolism and long-term outcome. JAMA. 2001; 286:2120–2127. [PubMed: 11694153]
4. Hoffman JM, Welsh-Bohmer KA, Hanson M, Crain B, Hulette C, Earl N, et al. FDG PET imaging in patients with pathologically verified dementia. J Nucl Med. 2000; 41:1920–1928. [PubMed: 11079505]
5. Detre JA, Leigh JS, Williams DS, Koretsky AP. Perfusion imaging. Magn Reson Med. 1992; 23:37–45. [PubMed: 1734182]
6. Wolf RL, Detre JA. Clinical neuroimaging using arterial spin-labeled perfusion magnetic resonance imaging. Neurotherapeutics. 2007; 4:346–359. [PubMed: 17599701]
7. Raichle ME. Behind the scenes of functional brain imaging: a historical and physiological perspective. Proc Natl Acad Sci USA. 1998; 95:765–772. [PubMed: 9448239]
8. Alsop DC, Dai W, Grossman M, Detre JA. Arterial Spin Labeling Blood Flow MRI: Its Role in the Early Characterization of Alzheimer's Disease. J Alzheimers Dis. 2010
9. Alsop DC, Detre JA, Grossman M. Assessment of cerebral blood flow in Alzheimer's disease by spin-labeled magnetic resonance imaging. Ann Neurol. 2000; 47:93–100. [PubMed: 10632106]
10. Asllani I, Habeck C, Scarmeas N, Borogovac A, Brown TR, Stern Y. Multivariate and univariate analysis of continuous arterial spin labeling perfusion MRI in Alzheimer's disease. J Cereb Blood Flow Metab. 2008; 28:725–736. [PubMed: 17960142]
11. Dai W, Lopez OL, Carmichael OT, Becker JT, Kuller LH, Gach HM. Mild cognitive impairment and Alzheimer disease: patterns of altered cerebral blood flow at MR imaging. Radiology. 2009; 250:856–866. [PubMed: 19164119]
12. Schuff N, Matsumoto S, Kmiecik J, Studholme C, Du A, Ezekiel F, et al. Cerebral blood flow in ischemic vascular dementia and Alzheimer's disease, measured by arterial spin-labeling magnetic resonance imaging. Alzheimers Dement. 2009; 5:454–462. [PubMed: 19896584]
13. Yoshiura T, Hiwatashi A, Yamashita K, Ohyagi Y, Monji A, Takayama Y, et al. Simultaneous measurement of arterial transit time, arterial blood volume, and cerebral blood flow using arterial spin-labeling in patients with Alzheimer disease. AJNR. 2009; 30:1388–1393. [PubMed: 19342545]
14. Raji CA, Lee C, Lopez OL, Tsay J, Boardman JF, Schwartz ED, et al. Initial experience in using continuous arterial spin-labeled MR imaging for early detection of Alzheimer disease. AJNR. 2010; 31:847–855. [PubMed: 20075093]
15. Newberg AB, Wang J, Rao H, Swanson RL, Wintering N, Karp JS, et al. Concurrent CBF and CMRGlc changes during human brain activation by combined fMRI-PET scanning. NeuroImage. 2005; 28:500–506. [PubMed: 16084114]
16. Morris JC, Weintraub S, Chui HC, Cummings J, Decarli C, Ferris S, et al. The Uniform Data Set (UDS): clinical and cognitive variables and descriptive data from Alzheimer Disease Centers. Alzheimer Dis Assoc Disord. 2006; 20:210–216. [PubMed: 17132964]
17. Mugler JP 3rd, Brookeman JR. Three-dimensional magnetization-prepared rapid gradient-echo imaging (3D MP RAGE). Magn Reson Med. 1990; 15:152–157. [PubMed: 2374495]
18. Wang J, Alsop DC, Song HK, Maldjian JA, Tang K, Salvucci AE, et al. Arterial transit time imaging with flow encoding arterial spin tagging (FEAST). Magn Reson Med. 2003; 50:599–607. [PubMed: 12939768]
19. Jagust WJ, Bandy D, Chen K, Foster NL, Landau SM, Mathis CA, et al. The Alzheimer's Disease Neuroimaging Initiative positron emission tomography core. Alzheimers Dement. 2010; 6:221–229. [PubMed: 20451870]
20. Erkinjuntti T, Gao F, Lee DH, Eliasziw M, Merskey H, Hachinski VC. Lack of difference in brain hyperintensities between patients with early Alzheimer's disease and control subjects. Arch Neurol. 1994; 51:260–268. [PubMed: 8129637]
21. Hanley JA, McNeil BJ. The meaning and use of the area under a receiver operating characteristic (ROC) curve. Radiology. 1982; 143:29–36. [PubMed: 7063747]

22. Hanley JA, McNeil BJ. A method of comparing the areas under receiver operating characteristic curves derived from the same cases. Radiology. 1983; 148:839–843. [PubMed: 6878708]

23. DeLong ER, DeLong DM, Clarke-Pearson DL. Comparing the areas under two or more correlated receiver operating characteristic curves: a nonparametric approach. Biometrics. 1988; 44:837–845. [PubMed: 3203132]

24. Alavi A, Newberg AB, Souder E, Berlin JA. Quantitative analysis of PET and MRI data in normal aging and Alzheimer's disease: atrophy weighted total brain metabolism and absolute whole brain metabolism as reliable discriminators. J Nucl Med. 1993; 34:1681–1687. [PubMed: 8410281]

25. Vaishnavi SN, Vlassenko AG, Rundle MM, Snyder AZ, Mintun MA, Raichle ME. Regional aerobic glycolysis in the human brain. Proc Natl Acad Sci USA. 2010; 107:17757–62. [PubMed: 20837536]

26. Vlassenko AG, Vaishnavi SN, Couture L, Sacco D, Shannon BJ, Mach RH, et al. Spatial correlation between brain aerobic glycolysis and amyloid-{beta} (A{beta}) deposition. Proc Natl Acad Sci USA. 2010; 107:17763–7. [PubMed: 20837517]

27. Jack CR Jr. Bernstein MA, Borowski BJ, Gunter JL, Fox NC, Thompson PM, et al. Update on the magnetic resonance imaging core of the Alzheimer's disease neuroimaging initiative. Alzheimers Dement. 2010; 6:212–220. [PubMed: 20451869]

28. Hu WT, Wang Z, Lee VM, Trojanowski JQ, Detre JA, Grossman M. Distinct Cerebral Perfusion Patterns in FTLD and AD. Neurology. 2010 in press.

29. Mosconi L, Sorbi S, de Leon MJ, Li Y, Nacmias B, Myoung PS, et al. Hypometabolism exceeds atrophy in presymptomatic early-onset familial Alzheimer's disease. J Nucl Med. 2006; 47:1778–1786. [PubMed: 17079810]

30. Mosconi L, Mistur R, Switalski R, Brys M, Glodzik L, Rich K, et al. Declining brain glucose metabolism in normal individuals with a maternal history of Alzheimer disease. Neurology. 2009; 72:513–520. [PubMed: 19005175]

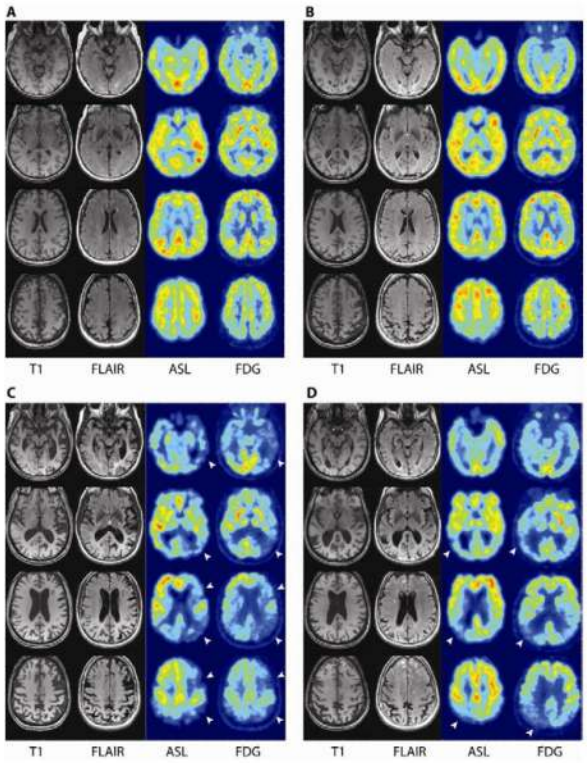

Figure 1.
Comparison of ASL and FDG images. Representative images from control (A&B) and AD patients (C&D) comparing structural MRI images (T1 and FLAIR), ASL-MRI, and FDG-PET. All four patients were diagnosed correctly by both readers using both modalities. White arrows highlight areas of concordant hypometabolism on FDG-PET and hypoperfusion on ASL-MRI.

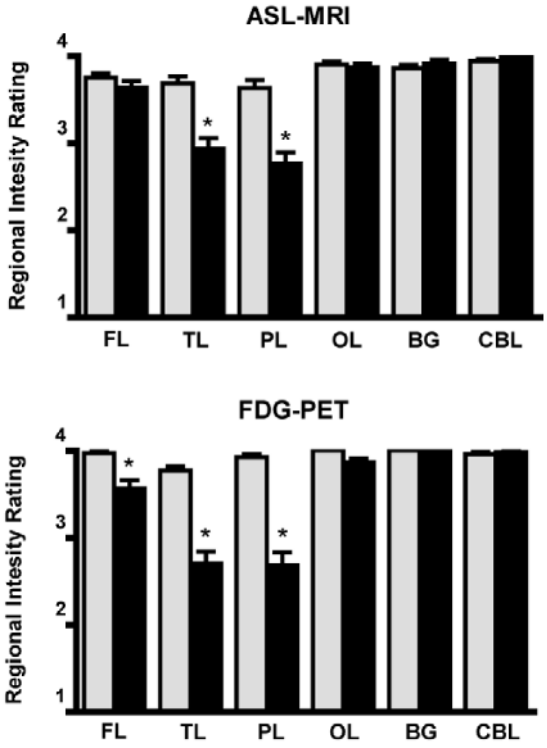

Figure 2.
Qualitative assessment of brain regional image intensity. Each image was scored from 1-4 (1 = severe hypointensity, 4 = normal). The pooled average of right and left for both readers is shown. Grey bars are control, black bars are AD. *p<0.01 vs. regional control by one-way ANOVA. FL: frontal lobe, TL: temporal lobe, PL: parietal lobe, OL: occipital lobe, BG: basal ganglia, CBL: cerebellum.

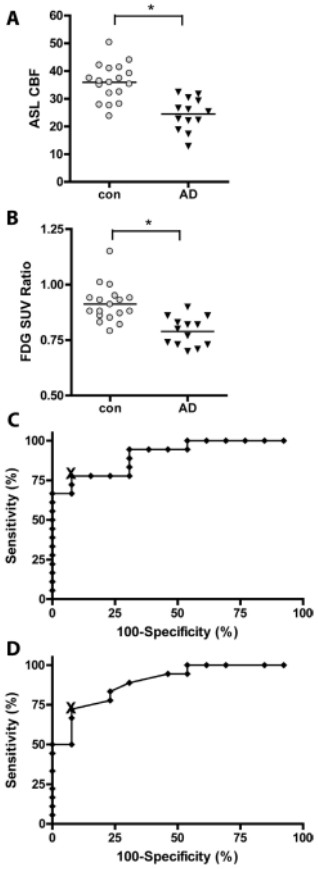

Figure 3.

Quantitative measures of global cerebral perfusion and metabolism. The ASL CBF (A) and FDG SUV ratio (B) data for AD patients (black triangles) and controls (grey circles) are compared. In both cases, AD was significantly different than control (*p<0.001 by unpaired 2-tailed t-test). ROC curves were constructed for ASL CBF (C) and FDG SUV ratio (D) data. The cutoff points for sensitivity/sensitivity calculation are marked with an "x". The area under the curve (AUC) values were 0.91 for ASL (standard error 0.053, p<0.001) and 0.90 for FDG (standard error 0.055, p<0.001).

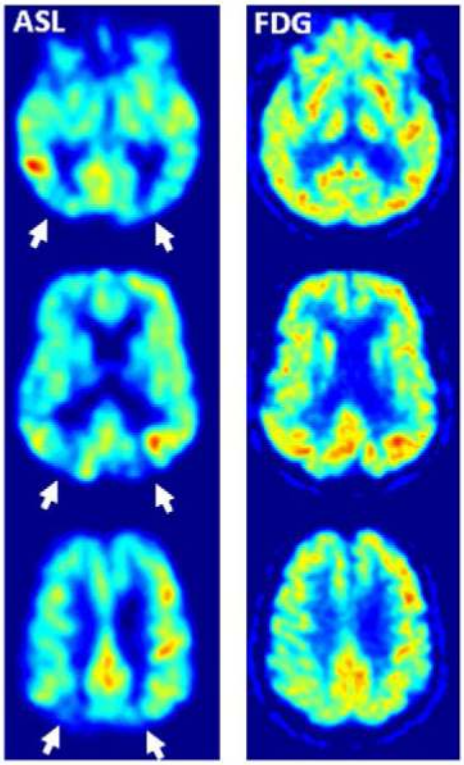

Figure 4.
Parieto-occipital hypoperfusion artifact on ASL-MRI. ASL-MRI images (left) from patient 9 (control) show areas of hypoperfusion in the parietal-occipital junction (arrows) that were not present on FDG-PET images (right). These were present in 4 control patients and are a potential source of diagnostic error.

Alzheimers Dement. Author manuscript; available in PMC 2013 January 01.

Table 1

Demographic, clinical, qualitative, and quantitative image analysis data. % difference indicates the % change from control. Age is in years, CBF in ml/100g*min, FDG SUV ratio in arbitrary units. 0= control, 1= AD.

				FDG-PET Read		ASL-MRI Read			
Subject#	**Diagnosis**	**Age**	**MMSE**	**Reader 1**	**Reader 2**	**Reader 1**	**Reader 2**	**ASL_CBF**	**FDG_Ratio**
1	0	59	29	0	0	0	0	30.27	*
3	0	74	30	0	0	1	0	39.12	0.85
4	0	68	30	0	0	0	0	32.42	1.15
5	0	65	30	0	0	0	0	50.32	0.88
6	0	76	30	0	0	0	0	37.38	0.86
7	0	75	28	1	0	0	0	42.07	0.88
9	0	73	30	0	0	1	0	27.84	0.93
12	0	73	30	0	0	0	0	28.12	0.82
13	0	53	30	0	0	0	0	36.36	0.94
17	0	76	30	0	0	0	0	35.30	0.83
19	0	61	29	0	0	0	0	40.90	0.93
20	0	76	30	0	0	0	0	43.99	1.00
21	0	68	27	0	0	0	0	35.05	0.91
23	0	61	28	0	0	0	0	41.35	0.94
24	0	69	30	1	0	0	1	23.72	0.79
25	0	58	29	0	0	0	0	37.31	0.95
27	0	80	28	0	0	0	0	27.58	0.88
29	0	70	30	0	0	0	0	35.91	1.01
30	0	78	29	0	0	0	0	31.98	0.87
Average + SD:		**69.1±7.7**	**29.3±0.9**					**35.6±6.6**	**0.91±.08**
2	1	75	22	1	0	0	0	34.47	*
8	1	60	16	1	1	1	0	30.41	0.73
10	1	64	2	1	1	1	1	17.34	0.86
11	1	66	25	**	**	1	1	25.08	*
14	1	74	21	1	1	1	0	22.40	0.82

				FDG-PET Read		ASL-MRI Read			
Subject#	**Diagnosis**	**Age**	**MMSE**	**Reader 1**	**Reader 2**	**Reader 1**	**Reader 2**	**ASL_CBF**	**FDG_Ratio**
15	1	77	23	1	1	1	1	12.90	0.70
16	1	77	20	1	1	***	***	***	0.74
18	1	74	15	1	1	1	1	18.90	0.74
22	1	67	17	1	1	1	1	32.44	0.71
26	1	77	23	1	1	1	1	22.16	0.86
28	1	67	24	1	1	1	0	26.22	0.83
31	1	77	20	0	0	1	1	29.34	0.80
32	1	74	20	0	0	1	0	22.77	0.73
33	1	78	7	1	1	1	1	19.61	*
34	1	80	24	0	0	0	0	26.65	0.77
35	1	78	25	1	0	0	0	31.73	0.90
36	1	76	24	0	0	1	0	25.44	0.82
Average ± SD:		**73.0±5.9**	**19.3±6.4**					**24.9±6.0**	**0.79±.06**
% difference		5.6	34.1					30.1	13.2
p value		0.10	**<0.001**					**<0.001**	**<0.001**

*FDG ratio could not be calculated due to technical issues (no SUVs).

**No FDG-PET images due to movement artifact.

***No ASL-MRI images due to movement artifact.